Available online at www.sciencedirect.com
SCIENCE DIRECT®
Journal of Sound and Vibration 279 (2005) 1181–1194
JOURNAL OF SOUND AND VIBRATION
www.elsevier.com/locate/jsvi

Short Communication

Evaluation of the damping ratio for a base-excited system by the modulations of responses

Wenlung Li*

Department of Mechanical Engineering, National Taipei University of Technology, Chung Hsiao E Road, Taipei 10626, Taiwan

Received 28 April 2003; accepted 21 January 2004
Available online 12 September 2004

Abstract

The present article gives a method for evaluating or identifying the linear viscous damping ratio of single-degree-of-freedom systems, which are excited from its base. Unlike most of the existing methods that are based on transient responses and the assumption of small damping, the present method does not require the system to have a small damping. The novel method is derived using the input-forcing function as the reference signal, and the corresponding system responds as the modulator. However, in order to get the phase-lag signal without measuring the amplitudes of input and response, a second reference signal has been proposed in the present report. That is, the input-forcing function with 90° shift in its phase is taken as the second reference. The two modulated signals are then independently split into two parts. The part, which is time-invariant, is the one containing the system damping. It has been shown by the numerical simulations that the given method identifies the damping ratio with a good accuracy if the excitation frequency is tuned to the phase-sensitive region. Finally, the experimental study in the present report also further substantiates the applicability and validity of the method.

1. Introduction

Friction or retarding force, damping as well as energy dissipation have been noticed long before 4 B.C. [1]. However, 2000 years later, topics related to damping, damping models, and damping

*Tel.: +886-2-2771-2171x2023; fax: +886-2-2731-7191.
E-mail address: wlli@ntut.edu.tw (W. Li).

0022-460X/$ - see front matter © 2004 Elsevier Ltd. All rights reserved.
doi:10.1016/j.jsv.2004.01.027

Nomenclature

a_0	dc of $g(t)$
b_0	dc of $\tilde{g}(t)$
c	damping
f_s	signal sampling frequency in Hz
$g(t)$	modulated response in time domain $= u(t)\,z(t)$
$\tilde{g}(t)$	the second modulated time response
G_0	measured $\tan\phi$
k	stiffness
m	mass
n	number of points of a sampled signal
Q	quality factor
r	frequency ratio $= \Omega/\omega_n$
r_d	frequency ratio $= \Omega/\omega_d$
r_z	amplitude transmissibility $= Z/U$
r_0	frequency ratio where $\phi = \pi/2$
Δt_s	sampling resolution $= 1/f_s$
$u(t)$	base excitation
U	amplitude of base excitation
$z(t)$	system responses in time domain
Z	amplitude of the system response
ϕ	lag angle due to system damping
ω_n	natural frequency in rad/s
Ω	excitation frequency in rad/s
Ω_0	excitation frequency at $\phi = \pi/2$
ζ	damping ratio
$\hat{\zeta}$	estimated damping ratio

control, etc. are still important and relevant to industrial practices. In addition, as it is well known, damping or friction actually induced vibration and a lot of nonlinear dynamic phenomena [2]. Moreover, due to the increasing complexity of modern technology, a method that can accurately represent the damping of a system is essential. In fact, it was Rayleigh [3] who was the first to precisely notice that the dissipative energy resulting from damping is proportional both to mass and velocity of a system. The energy dissipative function he proposed in the 19th century, is still commonly adopted in dynamic analysis today.

Unlike mass and stiffness properties, which can be directly measured or analytically computed by numerical models such as the finite element, the damping of a system is extremely difficult to obtain. Generally, the damping characteristics, no matter whether they are internal (e.g., material, micro-structural effects, friction, etc.) or external (e.g., boundary, fluid contact, fluid/structure interaction, etc.), can be revealed only by experimental measurement. Therefore, reasonably accurate identification methods that correlate the analytical model with measured data are important and necessary. In fact, there exist many models for various fields. For example, Ibrahim [4], Armstrong-Helouvry et al. [5] provided detailed surveys from the viewpoint of models, control and compensation. However, most of the given mathematical models are usually too complicated to be applied in tests. In addition, damping was clearly not as simple as the commonly used models would imply.

During the last couple of decades, research interests in damping or friction have been mostly focused in multi-degree-of-freedom (mdof) or nonlinear systems. For example, the reports from Refs. [6–8] provided several useful damping models for mdof based on non-negative energy dissipation functions, e.g., an exponentially decaying function. And the damping behavior was assumed to follow that exponential relaxation function, which is controlled by a so-called relaxation time constant. The main issue was then concentrated to fit the function by tuning the constant with experimental measurements. The results showed the models are good for both viscously and non-viscously damped systems. However, most reports [6–9] still

limit the system damping to be small in order to assure the accuracy. Or, the methods may lack uniqueness [10].

In order to estimate or measure the system damping (or damping ratio), several means have been developed. Some are documented in Refs. [9,11–13] for various systems. Essentially, all methods are theoretically based on the fact that the system damping has the property of decreasing the response amplitude. Therefore, one is to measure the damping ratio from the transient response and when the system is in free vibration. These methods include the method of logarithmic decrement, the quality factor or Q-factor method, curve fitting methods, etc. Again, these methods are based on the small damping assumption. Otherwise, the measurement error would be large.

Unlike those techniques only valid under the assumption of small damping, the recently proposed method by Li [14] is very accurate. And, the method derived in Ref. [14] only valid for systems that are directly excited by forcing functions. However, it may have circumstances that are impossible to apply forcing function directly on to the system during experiments. For example, the cantilever in front of a probe of an atomic force microscope can be modeled only by a base-excited system. And, it may be difficult to apply an external force on to the cantilever directly. Motivated by this, a novel idea is given in the present paper.

2. Derivation of the method

Refer to Fig. 1 for the responses of a linear sdof system, which is excited by $u(t)$ from its base can be represented by

$$m\ddot{z} + c(\dot{z} - \dot{u}) + k(z - u) = 0, \tag{1}$$

where m, c, and k are the equivalent mass, linear damping and stiffness of the system, respectively. If the base excitation satisfies

$$u(t) = U\mathrm{e}^{\mathrm{i}\Omega t} \tag{2}$$

in which $\mathrm{i} = \sqrt{-1}$, the steady-state solution of the mass can be obtained in terms of the complex form

$$z(t) = \left[\frac{1 + \mathrm{i}(2r\zeta)}{(1 - r^2) + \mathrm{i}(2r\zeta)}\right] U\mathrm{e}^{\mathrm{i}\Omega t} = Z\mathrm{e}^{\mathrm{i}(\Omega t - \phi)} \tag{3}$$

with

$$Z = r_Z \cdot U \tag{4}$$

and

$$\tan\phi = \frac{2\zeta r^3}{(1 - r^2) + (2r\zeta)^2}. \tag{5}$$

The symbols in Eq. (3) are defined in terms of the system parameters

$$\varsigma = \frac{c}{2\sqrt{mk}}, \quad r = \frac{\Omega}{\omega_n} \quad \text{and} \quad \omega_n^2 = \frac{k}{m}. \tag{6}$$

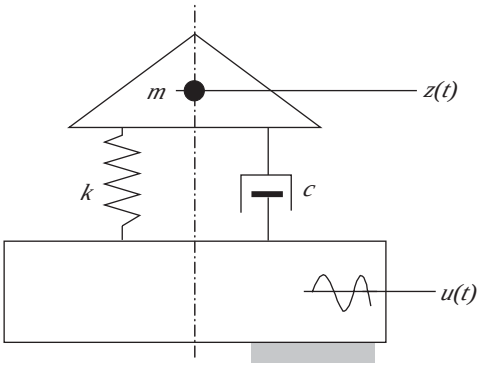

Fig. 1. Schematic diagram of a base-excited system.

Note, r_Z in Eq. (4) is called the transmissibility to denote the portion of the input amplitude that has been transmitted to the output. In fact, this transmissibility can be defined from Eq. (3) and has the form

$$r_Z = \left[\frac{1 + (2\zeta r)^2}{(1 - r^2)^2 + (2\zeta r)^2}\right]^{1/2}. \tag{7}$$

Without loss of the generality, in case the excitation is harmonic in an experiment, or

$$u(t) = U \sin(\Omega t), \tag{8}$$

then one has no difficulty to express $z(t)$ as

$$z(t) = Z \sin(\Omega t - \phi) \tag{9}$$

from Eq. (3). Applying the concept similar to that given in Ref. [14], one is able to define a response modulation function

$$g(t) = u(t) \cdot z(t) = U \sin(\Omega t) \cdot Z \sin(\Omega t - \phi), \tag{10}$$

in which $z(t)$ is taken as the modulator and $u(t)$ as the reference. Clearly, one may also equivalently write Eq. (10) as

$$g(t) = \frac{r_Z \cdot U^2}{2} [\cos\phi - \cos(2\Omega t - \phi)] \tag{11}$$

if the transmissibility is known. Notice that the first term of Eq. (11) is time-invariant, while the second has the frequency of 2Ω. In order to get the first term, one may simply design a low-pass filter (LPF) to get rid of the signal that has frequency of 2Ω in a vibration test. Thus, one has the time-invariant part

$$\|g(t)\|_{\mathrm{LPF}} = \frac{r_Z \cdot U^2}{2} \cos\phi, \tag{12}$$

where $\| \ldots \|$ denotes the filtered value. Equivalently, for the discrete signals, one has

$$a_0 = \|g(t)\|_{\mathrm{LPF}} \cong \frac{1}{n} \sum_{i=1}^{n} g(i \cdot \Delta t_s) \tag{13}$$

with $\Delta t_s = (1/f_s)$ and f_s is the sampling frequency and $\Delta t_s < T/2$, where T is the period of the excitation. Readers may refer to Ref. [14] for the detail discussion in this equivalence.

In the mean time, it is also possible to consider the input excitation with a $T/4$ or $\pi/2$ phase shift as the second reference of the response $z(t)$. By doing so, one can define the second response modulation as

$$\tilde{g}(t) = u(t - T/4) \cdot z(t) = \frac{r_Z \cdot U^2}{2} [\sin\phi - \sin(2\Omega t - \phi)], \tag{14}$$

and

$$b_0 = \|\tilde{g}(t)\|_{\mathrm{LPF}} = \frac{r_Z \cdot U^2}{2} \sin\phi \tag{15}$$

following the same procedure as Eq. (12). Therefore, one is able to evaluate $\tan\phi$ from the two filtered response modulations, or

$$G_0 = \frac{b_0}{a_0} = \frac{\|\tilde{g}(t)\|_{\mathrm{LPF}}}{\|g(t)\|_{\mathrm{LPF}}} = \frac{2\zeta r^3}{(1 - r^2) + (2r\zeta)^2}. \tag{16}$$

That is, Eq. (16) just takes the ratio of the two filtered signals to approximate $\tan\phi$ of Eq. (5). Fig. 2 depicts the schematic diagram for the electronic set-up of the idea. Note also that if r approaches 1.0 and ζ is fixed and small, then $G_0 \cong Q$, i.e., $\lim_{r\to 1} G_0 = Q$, where Q is the quality factor of the system. However, if ζ increases or r has a value other than 1.0, G_0 may have values far away from Q.

Examining Eq. (16), the transmissibility need not be known beforehand as it can cancel out each other in the equation. Besides, G_0 strongly depends only on the excitation frequency, which appears in r of the equation, but not on of the amplitude of its base excitation. As the consequence, the amplitude of the base excitation can be set just large enough to get the good quality responses during experiments. However, the merit of Eq. (15), which is with U^2, is to minimize the measurement error when ϕ is away from $\pi/2$ in which $\sin\phi$ alone is small and difficult to measure correctly.

Note that the signs of $\|g(t)\|_{\mathrm{LPF}}$ (a_0) and $\|\tilde{g}(t)\|_{\mathrm{LPF}}$ (b_0) are also important indices to delve into the true system damping. In case the experiment is carried out and gets $\phi < \pi/2$, then both a_0 and b_0 shall be positive. On the other hand, the sign of the former together with G_0 should change to negative while the latter keeps its sign positive if $\phi > \pi/2$. Otherwise, the error of evaluation is large, or the evaluated damping ratio cannot be trusted. Refer to Fig. 3 for this argument and the sign change of G_0.

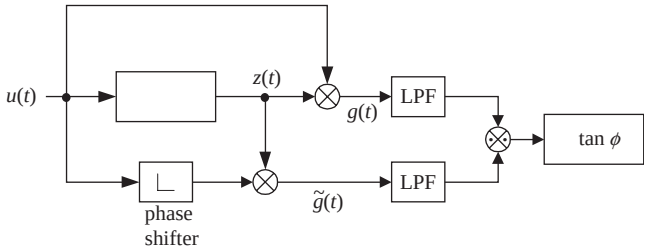

Fig. 2. Block diagram of electronic setup to get $\tan\phi$ from measurement.

Comparing Eq. (16) with (12), it is quite clear that the most sensitive regions for amplitudes and phases are not the same if damping ratios are not small. The maximum value for r_z always appears at $r<1.0$, while that of phases appears at the condition which satisfies the denominator of G_0 equal to zero or a small value. That is from Eq. (16), if the system damping ratio ζ satisfies

$$\varsigma_0 = \frac{\sqrt{r^2-1}}{2r} \quad \text{or} \quad r_0 = \frac{1}{\sqrt{1-4\zeta^2}}, \tag{17}$$

then G_0 has the maximum value. The subscripts of ζ_0 and r_0 are to denote the location that the phase lag is right at $\pi/2$. Certainly, condition (17) is true only when cases $r>1.0$. Besides, for every $\zeta<0.5$, there exists a corresponding r such that Eq. (17) being satisfied. In case condition (17) holds, then G_0 reaches its maximum value and the phase lag $\phi=\pi/2$, as shown in Fig. 3 by the heavy dotted line. Therefore, the location where the phase angle is most sensitive depends on both the excitation frequency and the system damping ratio. However, when the system damping is very small, this most-sensitive location is just slightly larger then $r=1.0$, or $r_0 \approx 1.0$. Furthermore, if $\zeta=0.5$, $r\to\infty$. Or, there exists no possible phase lag $\phi=\pi/2$.

Rearranging Eq. (16) and solving for ζ, one is able to write the damping ratio as

$$\hat{\zeta} = \frac{r^2 \pm \sqrt{r^4 - 4G_0^2(1-r^2)}}{4rG_0}, \tag{18}$$

in which the over-hat denotes the identified value. Since the damping ratio is real, the value computed from the square root must be real. Thus, the expression

$$\begin{aligned} &\frac{r^2}{2\sqrt{1-r^2}} > G_0 \quad \text{if } r<1.0, \\ &\frac{r^2}{2\sqrt{r^2-1}} < G_0 \quad \text{if } r>1.0 \end{aligned} \tag{19}$$

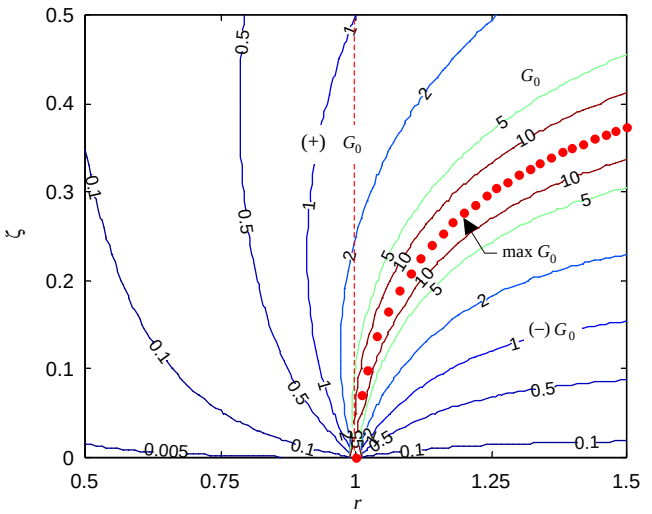

Fig. 3. Relation and sign change of G_0 on (r,ζ).

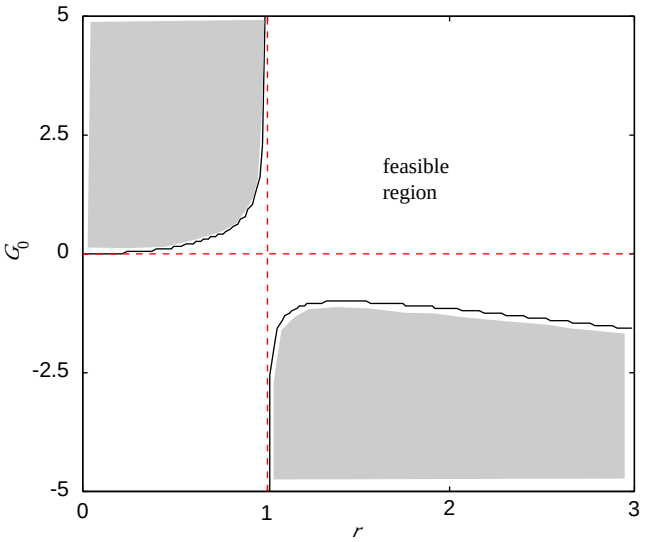

Fig. 4. Non-hatched area: feasible region for (r, G_0) combinations.

must be held in order to keep ζ real-valued. The feasible combinations for (r, G_0) are shown in Fig. 4. Meanwhile, it is also intrusive to keep only the positive root for the system damping ratio according to its definition.

3. Numerical verifications

In order to verify the validity of the damping identification method mentioned, numerical simulations have been conducted. Referring to Fig. 4, the frequency of base excitations should be selected close to the location where condition (17) holds or in the neighborhood of it so that better quality of the damping signals can be obtained. However, in order to show the validity of the present method, a wide range of excitation frequencies have been thoroughly studied.

For the first example, the parameters $\omega_n = 40\pi$ (or 20 Hz) and the sample frequency 500 Hz are used during the simulations while the amplitude of excitation is set to be unity. In addition, Eq. (13) is applied to compute the numerical average values, instead of a low-pass filter. The simulation results are shown in Fig. 5(a) for $\zeta = 0.01$, 0.05 and 0.1, respectively, which are considered as small damping. As one can read from the left corner of the figure, the sign check given in the last section provides a good tool to screen out negative damping ratios. However, Fig. 5(a) also indicates that the present method can correctly identify the system damping ratio only in the vicinity of $r \approx 1$. Other than this region, a large error has been noticed. The reason is quite clear. The energy transmitted from the base to the mass mainly through the mechanism of spring and mass effects in the region away from damping-sensitive region if damping is small. As a consequence, the phase-lag signal is relatively small, even negligible, comparing to its counter parts. Taking $\zeta = 0.05$ for example, the phase sensitivity, which is represented by $\tan\phi$ (or G_0) from Eq. (5), is less than 1.0 except at a small range near $r = 1$ ($r_0 = 1.005$), refer to Fig. 5(b).

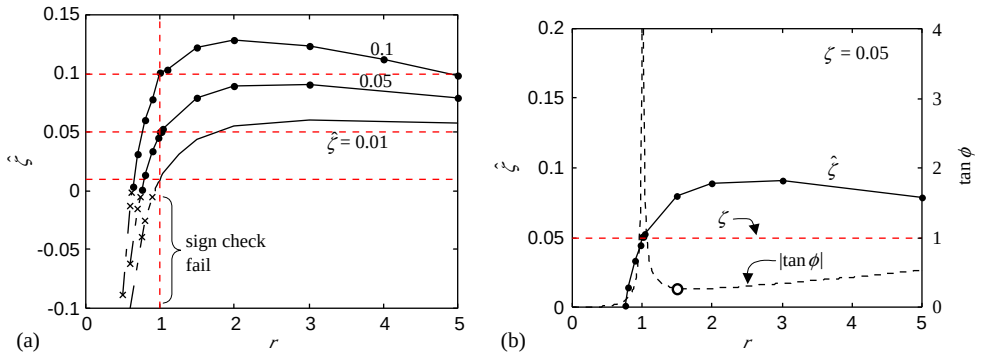

Fig. 5. Damping identification: numerical results for typical systems under base excitation.

Actually, the present method identifies the system damping correctly in the damping-sensitive region.

Fig. 6 shows the sign change of a_0, b_0 and G_0 for $\zeta = 0.1$ for various r's. It reveals that the part containing $\cos\phi$ decreases rapidly from positive to negative if r increases from a small value across the phase-sensitive region, while b_0 keeps its sign unchanged. However, the value of the latter also monotonically increases then decreases after $\phi = \pi/2$. These properties can be used to locate the bandwidth of the phase-sensitive region. Note also that the bandwidth of this region is inversely proportional to ζ. A smaller ζ results in a narrower bandwidth, which is defined as the frequency differences between $G_0 = \pm 1.0$ (Fig. 7), and a steeper slope of a_0 at the point (shown by 'O' in Fig. 6) it changes the sign. Thus, locating the phase-sensitive region could be crucial if ζ is small.

4. Experiments

In order to evaluate the damping ratio of a damped system from an experiment using the present method, one generally applies an excitation with the frequency right at one of the damped natural frequencies (ω_d) since ω_n may be not yet known. Thus, the practical frequency of the applied excitation is at

$$\omega_d = \omega_n\sqrt{1-\zeta^2} \quad \text{or} \quad r = \Omega/\omega_n = \sqrt{1-\zeta^2} \tag{20}$$

corresponding to a sdof system. Based on the conclusion given in the numerical simulation example, the oscillation frequency selected in accordance to Eq. (20) is certainly lower than the most sensitive range. However, it guarantees a high sensitivity in amplitudes. In addition this damped natural frequency can be easily found from many traditional experimental methods, like applying an impulse force through a hammer, or a sweep sine forcing function, etc.

Assuming that ζ at ω_d and Ω_0 are equal, it is possible to solve ω_n and ζ from Eqs. (17) and (20) from the measured Ω and ω_d, i.e.,

$$\hat{\zeta} = \left(\frac{5}{8} - \frac{1}{8r_d}\sqrt{16+9r_d^2}\right)^{0.5} \tag{21}$$

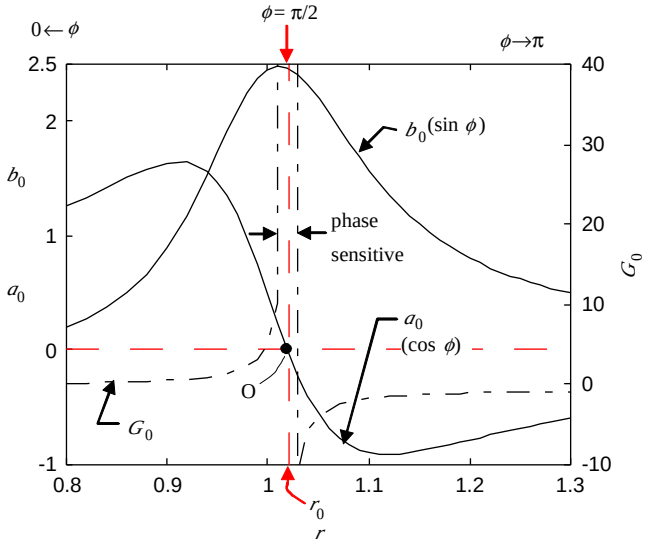

Fig. 6. Parameters a_0, b_0, and G_0 on various r's for $\zeta = 0.1$.

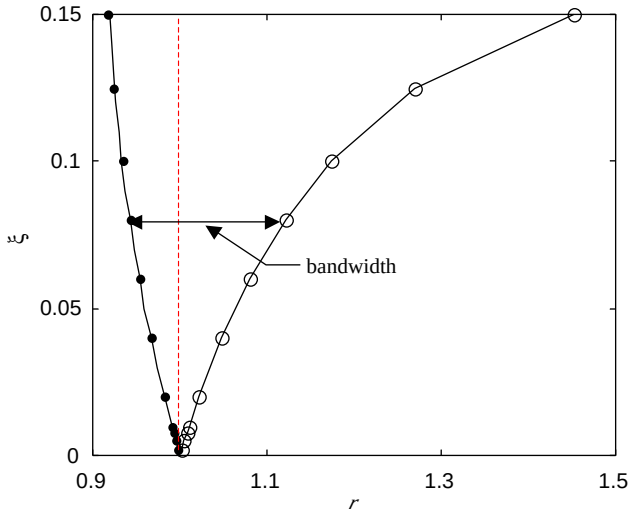

Fig. 7. The bandwidth of various ζ's for $|G_0| \geqslant 1$.

and

$$\hat{\omega}_n = \omega_d \left(-\frac{3r_d^2}{2} + \frac{r_d}{2}\sqrt{16 + 9r_d^2} \right)^{0.5} \tag{22}$$

where $r_d = \Omega_0/\omega_d$, where Ω_0 denotes the excitation frequency right at $\phi = \pi/2$. In general Ω_0 can be determined by evaluating a_0 through an experiment in such a way that letting $|a_0| < \varepsilon$, where ε is

an arbitrarily small and allowable tolerance. In addition, after examining Eqs. (17) and (20), one can easily conclude that

$$\omega_d \leqslant \omega_n \leqslant \Omega_0, \tag{23}$$

and the equality holds only when $\zeta = 0$, which is impossible for a practical system.

The experiment carried out to further verify the method is a cantilever beam system. The schematic diagram is shown in Fig. 8, in which a steel cantilever of dimension $1.7^{\mathrm{T}} \times 20.2^{\mathrm{W}} \times 240^{\mathrm{L}}$ mm (ca. 64.3 g) is directly mounted on to a shaker. Theoretically, the beam has the natural frequency at ca. 11.25 Hz. However, experimentally the damped natural frequency (ω_d) of the beam is found to be 12.695 ± 0.005 Hz with 90% confidence level, and $Q \approx 29$ when it oscillates in air.

During the experiments, the sampling frequency f_s has been set to 500 Hz. Sinusoidal excitations of various frequencies were applied from the controller to the shaker and detected by sensor 1 (S1) mounted on the base of the cantilever; see Fig. 8 for the detail set up. The system responses are then detected by sensor 2 (S2) which is located at the tip of the beam. Fig. 9 shows typical responses in the time and frequency domains. The result verified the validity of Eqs. (11) and (14) that predict the modulations containing both the time-invariant and signals of 2Ω.

Collecting a_0 and b_0 of the beam for different excitation frequencies in the neighborhood of $r = 1$, the results are plotted in Fig. 10. Each of data points shown in Fig. 10 is based on the average of 10 repeated measurements. The plot clearly indicates the sign change of a_0 that is predicted by the numerical simulation. Thus, using the idea of sign change on a_0 in Fig. 10, one is able to locate the approximate frequency that corresponds to $\phi = \pi/2$. In fact, that excitation frequency is Ω_0 in Eq. (22). Thus, one can obtain $\Omega_0 \approx 12.73$ Hz from the experimental data by curve-fitting, refer to Fig. 10. The measured system damping ratio as well as the natural frequency can be then correspondingly computed by applying Eqs. (21) and (22), respectively. The results are tabulated in Table 1. Table 1 also shows the results that in case the evaluated Ω_0 slightly deviates from 12.73 Hz. As it has been shown in the table, small deviation on Ω_0 causes relatively large change in ζ. Therefore, carefully measuring and lock-in the location of Ω_0 is required in order to get a more accurate damping ratio. In the meantime, the error of Ω_0 in the positive side or away from ω_d tends to identify a larger damping ratio. Actually, this result has been implicitly indicated in Eq. (23).

In order to further delve into the applicability of the present method, the experimental results from 12.5 to 13.0 Hz are tabulated in Table 2. Based on the conclusion from Table 1 that the natural frequency for the cantilever is 12.702 Hz ($\Omega_0 = 12.73$ Hz), they are all in the vicinity of $\phi = \pi/2$. Table 2 shows that the damping ratios evaluated by Eq. (18) are between 2.8% and 5.4%, and with an average of 4.2%. These values are somewhat different from that of Table 1, which has 3.3% (2.2–4.2%). In addition, the difference between the two damping ratios of the excitation frequencies (12.7 and 12.8 Hz) just next to the sign change of G_0 tends to be larger than others. These two frequency locations are supposed to be the most damping-sensitive. However, as far as the experimental results can conclude that they may have larger error. The main reason stems from the numerical manipulation of G_0 in the present experiments. Since the denominator (a_0) of G_0 is very close to zero, a small change in a_0 causes large variation in G_0. In case the experiment was carried out by directly implementing through the hardware given in Fig. 2, more accurate results would be expected.

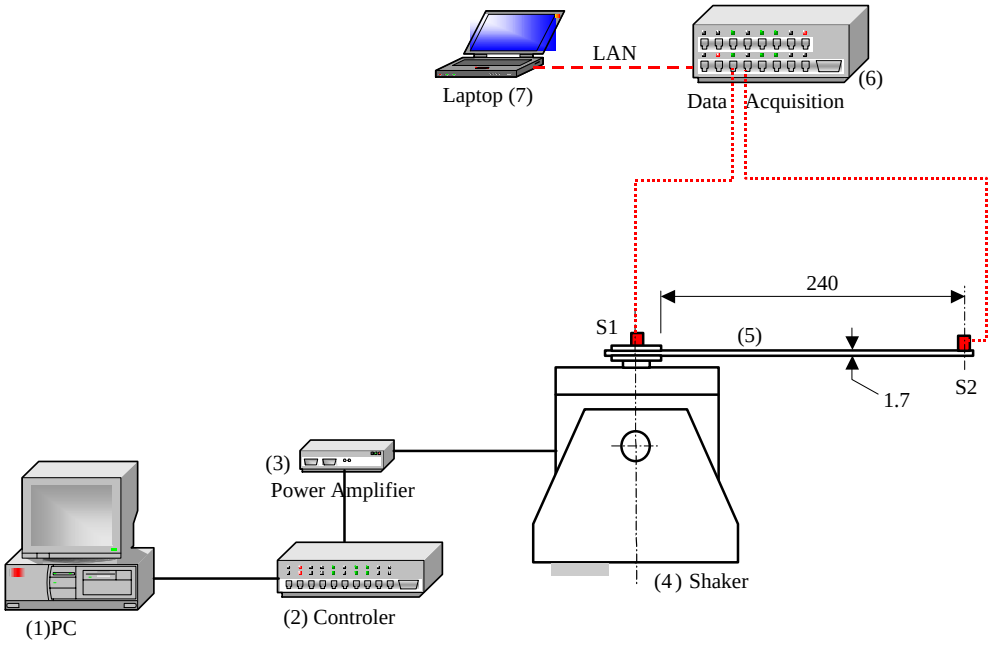

Fig. 8. The experimental setup (1: PC; 2: signal controller, Dactron; 3: power amplifier, B&K 2706; 4: exciter, B&K 4809, 5: cantilever; 6: acquisition system, iMC μ-Musys; 7: PC and software, FAMOS).

5. Conclusions

A novel evaluation method for the linear viscous damping of systems under base excitation is presented in this paper. The method is derived using the input-forcing function as the reference signal, and the system responses as the modulator. However, in order to get the phase-lag signal without measuring the amplitudes of the input and response, a second reference signal has been proposed in the present report. That is, the input forcing function shifted with 90° in its phase is taken as the second reference. The modulated signals are then filtered into two parts. The first part is time-invariant and contains information of the system. The second part relates to signals with high frequency. Therefore, the part with high frequency may be screened out by using a low-pass filter or by averaging a segment of the modulated signals. In addition to the derivation of the method, the region where a better quality of damping signal occurs is also discussed. Unlike the amplitude, which has the maximum always at its resonance, the phase-sensitive region is at slightly larger than the resonance depending on the system damping. Finally, the validity of the method is verified by numerical simulations. It has been shown that the given method identifies the damping ratio with good accuracy if the excitation frequency is tuned to inside the phase-sensitive region. Moreover, the method is also verified by the experimental study of a cantilever. Essentially, the experimental results substantiate the validity and applicability of the present method.

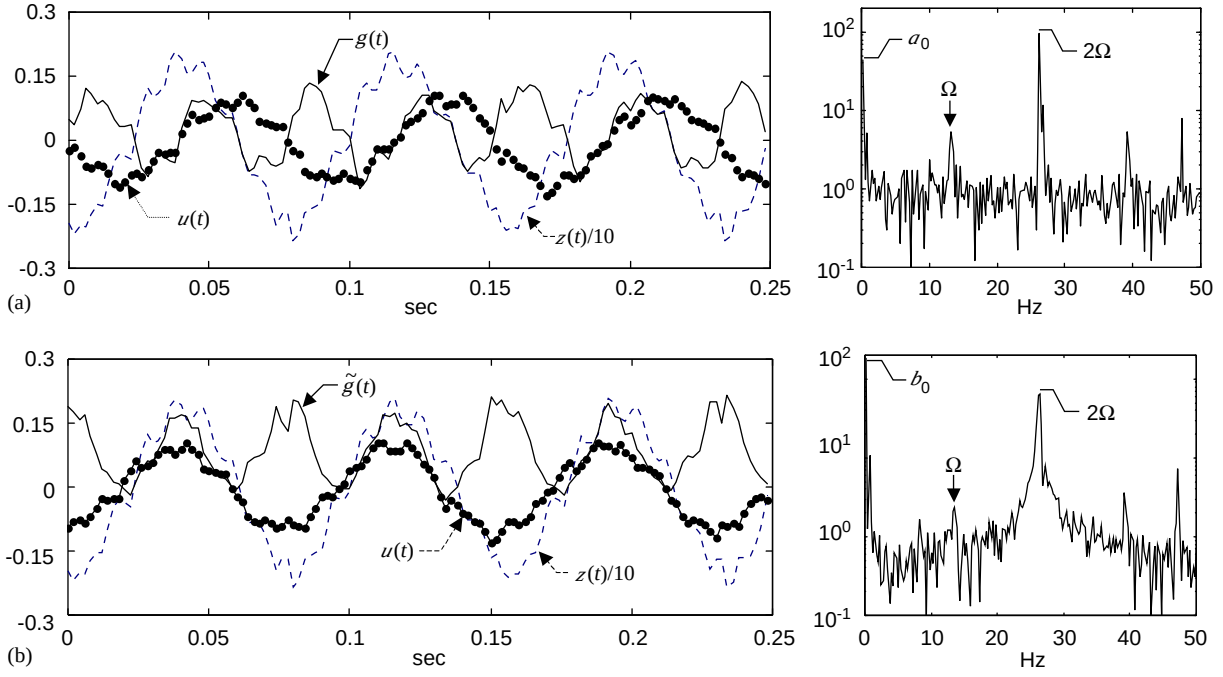

Fig. 9. Typical experimental results at $\Omega = 13\,\text{Hz}$: (a) $g(t)$; (b) $\tilde{g}(t)$. The frequency plots are the FFT of the corresponding $g(t)$.

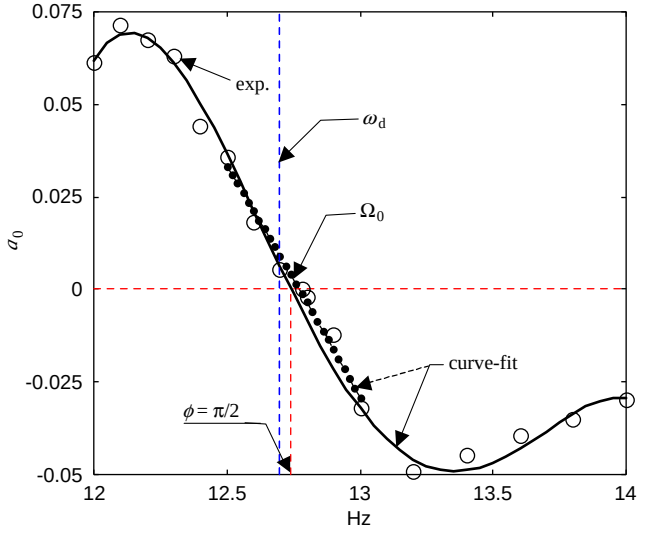

Fig. 10. a_0 at frequencies near ω_d (○: experiment; – and - -: curve-fitted).

Table 1
Comparisons for experimentally identified results

Medium	Ω_0 (Hz)	ω_n		ζ
		Eq. (24) $\hat{\omega}_n$ (Hz)	Theoretical[a] $\omega_{n,t}$ (Hz)	Eq. (23) $\hat{\varsigma}_2$ (%)
Air	12.73	12.702		3.3
	12.71	12.698	11.25	2.2
	12.75	12.706		4.2

[a] $\omega_{n,t} = \sqrt{k/m}$, $k = 3EI/l^3$.

Table 2
Evaluated ζ for the cantilever at 12.5–13 Hz

r $(\Omega/\hat{\omega}_n)$	Ω (Hz)	Sign of G_0	Eq. (18) $\hat{\varsigma}_1$ (%)	$0.5/Q$ $\hat{\varsigma}_3$ (%)
0.984	12.5	+	3.4	—
0.992	12.6	+	2.8	—
0.9998	12.7	+	3.8	1.7
1.008	12.8	−	5.3	—
1.016	12.9	−	5.4	—
1.024	13.0	−	4.2	—

References

[1] B. Feeny, A. Guran, N. Hinrichs, K. Popp, A historical review on dry friction and stick-slip phenomena, *Applied Mechanics Review* 51 (1998) 321–341.

[2] R.A. Ibrahim, Friction induced vibration, chatter, squeal and chaos—part I: mechanics of friction, *Applied Mechanics Review* 47 (1994) 209–226.

[3] J.W. Strutt, B. Rayleigh, *The Theory of Sound*, MacMillan, London, 1894 (reprint, 1944).

[4] R.A. Ibrahim, Friction induced vibration chatter squeal and chaos—part II: dynamics and modeling, *Applied Mechanics Review* 47 (1994) 227–253.

[5] B. Armstrong-Helouvry, P. Dupont, C.C. de Wit, A survey of models, analysis tools and compensation methods for the control of machines with friction, *Automatica* 30 (1994) 1083–1138.

[6] S. Adhikari, J. Woodhouse, Identification of damping—part 1: viscous damping, *Journal of Sound and Vibration* 243 (2001) 43–61.

[7] S. Adhikari, J. Woodhouse, Identification of damping—part 2: non-viscous damping, *Journal of Sound and Vibration* 243 (2001) 63–68.

[8] S. Adhikari, J. Woodhouse, Identification of damping—part 3: symmetry-preserving methods, *Journal of Sound and Vibration* 251 (2002) 477–490.

[9] D.I.G. Jones, *Viscoelastic Vibration Damping*, Wiley, New York, 2001.

[10] M.E. Gaylard, Identification of proportional and other sorts of damping matrices using a weighted response-integral method, *Mechanical Systems and Signal Processing* 15 (2) (2001) 245–256.

[11] K.G. Macconnell, *Vibration Testing, Theory and Practice*, Wiley, New York, 1995.
[12] D.J. Mead, *Passive Vibration Control*, Wiley, Chichester, 1998.
[13] J. Woodhouse, Linear damping models for structural vibration, *Journal of Sound and Vibration* 215 (1998) 547–569.
[14] W. Li, Continuous evaluation of viscous damping by the modulation of steady-state responses, *Proceedings of the 20th Conference on Mechanical Engineering*, vol. C, Taipei, Taiwan, 2003, pp. 553–558.